Electrical Engineering (2026) 108:137
https://doi.org/10.1007/s00202-025-03416-w

ORIGINAL PAPER

Cost-effective optimal hybrid active harmonic filter design to maximize loading capacity of power transformers in harmonic-rich systems

Alp Karadeniz[1] · Murat Erhan Balci[1] · Shady H. E. Abdel Aleem[2]

Received: 1 February 2025 / Accepted: 16 September 2025 / Published online: 20 January 2026

Abstract
This paper introduces an optimal design of the hybrid active filter combining a single-tuned passive filter and an active filter to cost-effectively improve the permissible loading capacity of power transformers operating in harmonic-rich systems. The proposed design method aims to minimize the harmonic loss factor (F_{HL}), the filter's investment cost, and the fundamental frequency loss in the active filter part. Its constraints include the individual and total harmonic distortion limitations specified by the IEEE standard 519, the desired displacement power factor interval, and the passive filter's quality factor range. To evaluate the performance of the proposed optimal design, particle swarm optimization and genetic algorithm methods are applied to two harmonic distortion scenarios within an industrial two-bus distribution system. Simulation results show that the proposed filter design significantly reduces harmonic distortions and the F_{HL} index, improving transformer loading capacity by rates of up to approximately 168%. In addition to that, the parametric analyses obtained in the Matlab/Simulink environment confirm the robustness of the design across varying loading and short-circuit impedance conditions.

Keywords Distorted systems · Hybrid active filters · Loading capacity · Optimal sizing · Power transformers

1 Introduction

The voltages and/or currents that deviate from sinusoidal waveforms are one of the major power quality problems in alternating current power systems. By expanding the non-sinusoidal waveforms into Fourier series, they can be expressed as a sum of sinusoidal components at frequencies that are multiples of the fundamental frequency. Each of the sinusoidal components is called a harmonic. Therefore, the non-sinusoidal voltages and currents are referred to as harmonically distorted voltages and currents in the literature [1].

Modern electric power networks increasingly feature renewable-based distributed generation units, such as wind turbines and photovoltaic power plants, alongside various nonlinear loads, including motor drives and computers. These power electronic circuit-based systems inherently distort voltage and current waveforms due to their nonlinear characteristics [2]. Harmonics adversely affect electrical networks and their components, leading to poor power factor, reduced efficiency, additional energy losses, lower permissible loading capacity, and shorter equipment lifespans [1].

It is well known in the literature that simple compensation capacitors can draw significantly distorted current harmonics in the harmonically distorted systems, thus worsening the voltage and current harmonic distortion in the system. As a result, to improve power factor and harmonic distortion in the distorted systems, passive and active filters are employed. Passive filters are cost-effective and simpler to install, whereas active filters provide superior harmonic mitigation performance. Hence, the hybrid active harmonic filters—which consist of passive and active filters—are chosen to provide cost-effective harmonic mitigation, particularly in high-power applications [3, 4]. Hybrid active harmonic filters have three main classes. These are a series active filter combined with a shunt passive filter, a shunt active filter combined with a shunt passive filter, and an active filter in series with a shunt passive filter [4, 5].

✉ Murat Erhan Balci
mbalci@balikesir.edu.tr

1 Department of Electrical and Electronics Engineering, Balikesir University, Balikesir, Türkiye

2 Department of Electrical Engineering, Institute of Aviation Engineering and Technology, Giza, Egypt

There are several passive filter types such as single-tuned, double-tuned, triple-tuned, damped double-tuned, and C-type filters [6]. Additionally, LCL filters are employed for the harmonic mitigation of the grid-connected converters [7]. Recently, several new passive filter topologies—such as the fully integrated T-LCL filter [8], magnetic integrated double-trap filter [9], magnetic integrated LLCL filter [10], and magnetic integrated multi-trap filters [11]—have also been studied for the reduction of switching harmonics generated by power converters widely used in traction systems. Another important motivation behind these designs is the reduction of filter size [9–11]. Although generally proposed for traction converters, such filters can also be used in various distribution networks including industrial power systems and renewable energy systems [10].

It is well known in the literature that the cost, losses, harmonic mitigation performance, and reactive power compensation capacity of passive filters can be affected by design parameters in contradictory ways. Therefore, their design is traditionally addressed in the literature as a single- or multi-objective optimization problem. The objectives commonly considered in these optimization approaches are the cost and/or loss minimization of the filter, the minimization of current and/or voltage harmonic distortions, and the maximization of the power factor [12]. Apart from these goals, references [13] and [14] present the optimal designs of C-type and single-tuned passive filters that aim to minimize the harmonic loss factor index (F_{HL}). Reference [13] also demonstrates that a passive filter design aimed at minimizing the F_{HL} index significantly differs from those based on conventional optimal design objectives. Since the F_{HL} index, defined in IEEE standard C57.110, is inversely proportional to the permissible loading capacity (S_{max}) of a power transformer operated under distorted voltages and currents, it can be mentioned that the goal of these two optimal filter designs is to maximize S_{max} in practice. Then, in [6], Karadeniz and Balci evaluate the performance of several passive filter types on the loading capacity maximization of a power transformer in a distorted system.

On the other side, the optimal sizing and placement studies of the active filters in the literature generally aim to minimize their current rating or cost while adequately reducing the voltage and current harmonic pollution [15]. In addition to that, in several studies [16–18], hybrid active filters are optimized to minimize the harmonic pollution index, which is the vector sum of the total voltage and total current harmonic distortion indices. In [19], Zobaa presents an optimal design of passive filter parameters to minimize the rating of the power converter in the hybrid active filter.

1.1 Aim of the work

The literature summary given above shows that there are few studies on the optimal passive filter design to maximize the transformer's loading capacity under nonlinear loading. Passive filters have limited capacity for mitigating harmonic distortion and increasing transformer loading capacity. Additionally, the sole use of active filters can be costly for high power ratings. As a result, it is seen that there is a need to propose an optimal hybrid filter design as a cost-effective solution to maximize the permissible loading capacity of transformers in highly distorted systems. However, there is no study on this issue.

In [20], Karadeniz and Balci identify this need and propose an optimization strategy for a hybrid filter design consisting of a shunt single-tuned passive filter and a shunt active filter. The objective of the strategy is to maximize the transformer's loading capacity while minimizing the filter's investment cost. The constraints include harmonic limitations defined in IEEE standard 519 [21] and the desired power factor range. However, in the design strategy, the minimization of the fundamental frequency loss in the active filter is not considered as a goal, and the quality factor range for the passive filter is not included among the constraints. These aspects are important for providing an energy-efficient hybrid filter. Additionally, in [20], the performance of the optimized hybrid filter is not examined under varying load demand or changes in the utility-side's short-circuit impedance. Finally, in the same study, the optimal design results are obtained solely using the particle swarm optimization (PSO) algorithm, without cross-validation using an alternative optimization method.

This study aims to address the gaps by reformulating the optimal hybrid filter design considering filter losses, evaluating its performance under varying consumer and utility conditions, and validating the results through a second optimization algorithm.

1.2 Contributions of the work to the literature

This work provides three major contributions to the literature. They can be mentioned as follows:

1. An optimal sizing approach is proposed to minimize an objective function including the investment cost of the hybrid active filter, the harmonic loss factor (F_{HL}), and the fundamental frequency loss of the active filter part. The constraints of the proposed optimal design are the individual and total harmonic distortion limitations specified by the IEEE standard 519, the desired interval of the displacement power factor (95% (lagging) < DPF < 100%), and the quality factor range of the passive filter part ($30 < Q < 60$).

2. For two harmonic-rich system scenarios, the optimal design results are obtained using the PSO algorithm [6, 22]. Subsequently, the performance of the proposed optimal hybrid active filter design is evaluated. The same design problem is also solved using the genetic algorithm (GA) [23–25], demonstrating that both algorithms yield highly comparable results. Since PSO and GA are widely known in the literature [22, 24] and successfully applied in various optimal passive filter design studies [6, 25], they are notably preferred in this study.
3. To evaluate the suitability of the proposed filter design for practical applications, a time-domain model of the system is developed in the Simulink environment. Using this model, the hybrid filter's performance is tested under a wide range of variations in load demand and the system's short-circuit impedance.

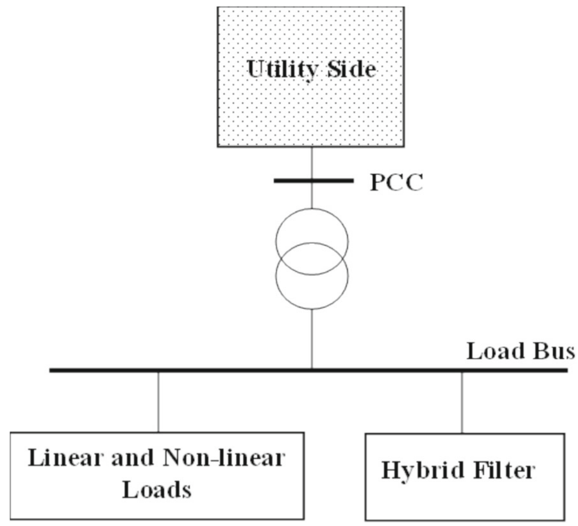

Fig. 1 The two-bus distribution system considered in the analysis

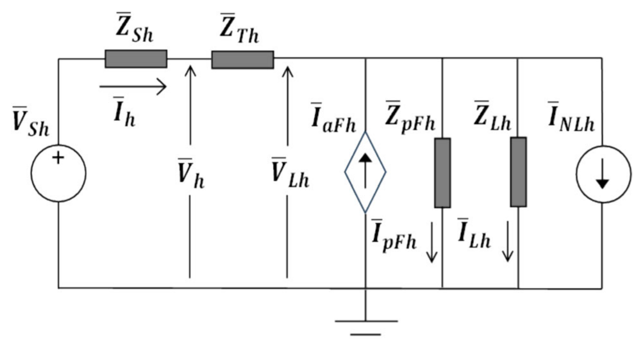

Fig. 2 The single-phase equivalent circuit of the system for hth harmonic order

1.3 Organization of the work

The work is organized into five sections. In Sect. 2, the system model in the harmonic domain is described in detail. Section 3 presents the problem formulation of the proposed design approach and a summary of PSO and GA techniques used for the solution of the problem. In Sect. 4, the performance of the optimal hybrid active filter is evaluated. Additionally, its effectiveness under variable loading and the system short-circuit impedance conditions is parametrically investigated using the time-domain model of the system in the Simulink environment. Finally, Sect. 5 summarizes key findings and conclusions of the study.

2 Modeling of the system in harmonic domain

To obtain the optimization results in this study, the hybrid active filter is inserted into the two-bus distribution system simulated in [6] instead of the passive filter. The one-line diagram of the modeled system is shown in Fig. 1. In the system, the load of the consumer includes three-phase balanced linear and nonlinear (harmonic-producing) loads. The power transformer is dedicated to supplying the consumer in the system. The hybrid active filter consists of a shunt active filter and a shunt single-tuned passive filter. The system's single-phase equivalent circuit is given in Fig. 2. Here it should be noted that superscript (¯) means the phasor value of the impedances, voltages, and currents in the equivalent circuit.

In the equivalent circuit, the utility side is modeled using a Thevenin voltage source, $\overline{V}_{\text{Sh}}$, and a Thevenin (or short-circuit) impedance, $\overline{Z}_{\text{Sh}}$, for each harmonic order [6]:

$$\overline{Z}_{\text{Sh}} = R_S + jhX_S \tag{1}$$

The power transformer can be represented using its winding resistance for the hth harmonic order (R_{Th}) and its fundamental frequency winding reactance (X_T), both referred to the primary side [6, 13, 26]:

$$\overline{Z}_{\text{Th}} = R_{\text{Th}} + jhX_T \tag{2}$$

Note that the hth harmonic equivalent resistance of the transformer windings can be calculated based on resistances related to its DC loss and fundamental frequency eddy current loss [13]:

$$R_{\text{Th}} = R_{\text{DC}} + h^2 R_{\text{ec}} \tag{3}$$

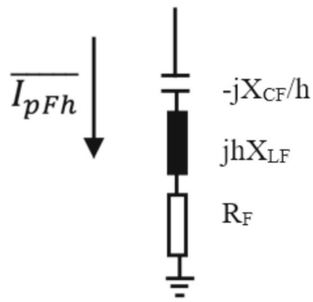

Fig. 3 The single-tuned filter's equivalent circuit

The linear and nonlinear load group is modeled in the equivalent circuit as the parallel connection of $\overline{Z}_{\mathrm{Lh}} = R_L + jhX_L$ and the harmonic current source, $\overline{I}_{\mathrm{NLh}}$. Note that the current harmonic source is one of the widely known models used for simulating the current distortion of the nonlinear loads in the literature [27].

For hth harmonic order, the single-phase circuit of the single-tuned passive filter is illustrated in Fig. 3, and the phasor value of its impedance can be calculated based on Eq. (4) [28, 29]:

$$\overline{Z}_{\mathrm{pFh}} = -j\frac{X_{\mathrm{CF}}}{h} + jhX_{\mathrm{LF}} + R_F \tag{4}$$

The relation among the fundamental frequency capacitive reactance (X_{CF}), fundamental frequency inductive reactance (X_{LF}), resistor (R_F), quality factor (Q), and tuned harmonic order (h_t) of the passive filter can be written as follows [28]:

$$h_t = \sqrt{\frac{X_{\mathrm{CF}}}{X_{\mathrm{LF}}}} \tag{5}$$

$$Q = \frac{h_t X_{\mathrm{LF}}}{R_F} \tag{6}$$

The shunt active filter can practically be represented as a current source in the equivalent circuit of the system. The current injected by the active filter into the system depends on the active compensation strategy. The active compensation strategies can be divided into three classes: (1) unity power factor, (2) constant instantaneous power, and (3) sinusoidal source current active compensation [30]. In this study, according to the first one, the current injected by the active filter is simulated.

To achieve unity power factor according to Fryze's power theory, for each phase, the waveform of the line current should be a replica of the load voltage's waveform, and they should also be in phase [31]. Thus, the instantaneous current synthesized by the active filter can be expressed using the load's equivalent conductance (G_e), instantaneous load current ($i_L(t)$), and instantaneous load voltage ($v_L(t)$) [31]:

$$i_{\mathrm{aF}}(t) = i_L(t) - G_e v_L(t) \tag{7}$$

Here it should be underlined that the load's equivalent conductance can be calculated using average power (P) and the square of true RMS voltage (V_L) at the load bus:

$$G_e = \frac{P}{V_L^2} = \frac{\sum_h V_{\mathrm{Lh}} I_h \cos(\theta_h)}{\sum_h V_{\mathrm{Lh}}^2} \tag{8}$$

where V_{Lh} and I_h are the rms values of the hth harmonic load voltage and hth harmonic line current and θ_h represents the phase angle difference between them. Moreover, for the system model shown in Fig. 2, the total instantaneous load current, $i_{\mathrm{L}}(t)$, is obtained in the time domain as the sum of three components: the current flowing through the passive filter impedance ($\overline{Z}_{\mathrm{pFh}}$), the current flowing through the load impedance ($\overline{Z}_{\mathrm{Lh}}$), and the time-domain equivalent of the harmonic current source, which directly injects current into the system ($\overline{I}_{\mathrm{NLh}}$).

Thus, the harmonic currents injected by the active filter can be rewritten in terms of the harmonic currents flowing through load impedance and passive filter ($\overline{I}_{\mathrm{Lh}}and\overline{I}_{\mathrm{pFh}}$), the harmonic currents generated by the load ($\overline{I}_{\mathrm{NLh}}$), G_e, $\overline{V}_{\mathrm{Lh}}$, and a scaling parameter (β):

$$\overline{I}_{\mathrm{aFh}} = \beta\left(\overline{I}_{\mathrm{Lh}} + \overline{I}_{\mathrm{NLh}} + \overline{I}_{\mathrm{pFh}} - G_e\overline{V}_{\mathrm{Lh}}\right) \tag{9}$$

where $\overline{I}_{\mathrm{Lh}}and\overline{I}_{\mathrm{pFh}}$ are calculated as follows:

$$\overline{I}_{\mathrm{Lh}} = \frac{\overline{V}_{\mathrm{Lh}}}{\overline{Z}_{\mathrm{Lh}}} \tag{10}$$

$$\overline{I}_{\mathrm{pFh}} = \frac{\overline{V}_{\mathrm{Lh}}}{\overline{Z}_{\mathrm{pFh}}} \tag{11}$$

Note that β controls the amount of reactive current generated by the active filter and can take values between 0 and 1. During the optimization process, G_e is not directly computed from Eq. (8), and it is considered as a tunable parameter to minimize the fundamental frequency loss of the active filter.

Concerning the equipment models detailed up to here, the node voltage method is implemented to express the harmonic components of the load voltage ($\overline{V}_{\mathrm{Lh}}$), line current ($\overline{I}_h$), and PCC voltage ($\overline{V}_h$) in the single-phase equivalent circuit:

$$\overline{V}_{\mathrm{Lh}} = \frac{1}{A_h}\left[\frac{\overline{V}_{\mathrm{Sh}}}{(\overline{Z}_{\mathrm{Sh}} + \overline{Z}_{\mathrm{Th}})} + (\beta - 1)\overline{I}_{\mathrm{NLh}}\right] \tag{12}$$

$$\underline{I}_h = \frac{\overline{V}_{\mathrm{Sh}} - \overline{V}_{\mathrm{Lh}}}{(\overline{Z}_{\mathrm{Sh}} + \overline{Z}_{\mathrm{Th}})} \tag{13}$$

$$\overline{V}_h = \overline{V}_{\mathrm{Sh}} - \overline{I}_h\overline{Z}_{\mathrm{Sh}} \tag{14}$$

where A_h is written as

$$A_h = \left[\frac{1-\beta}{\overline{Z}_{\text{pFh}}} + \frac{1-\beta}{\overline{Z}_{\text{Lh}}} + G_e\beta + \frac{1}{(\overline{Z}_{\text{Sh}} + \overline{Z}_{\text{Th}})} \right] \quad (15)$$

In this way, for the system, the harmonic distortion quantification indices can be computed:

- Total and individual voltage harmonic distortions at the PCC [6, 21]:

$$\text{THDV}(\%) = 100\frac{\sqrt{\sum_{h\geq 2} {V_h}^2}}{V_1} \quad (16)$$

$$V_h(\%) = 100\frac{V_h}{V_1} \quad (17)$$

- Total and individual current harmonic distortions of the line current [6, 21]:

$$\text{THDI}(\%) = 100\frac{\sqrt{\sum_{h\geq 2} {I_h}^2}}{I_1} \quad (18)$$

$$I_h(\%) = 100\frac{I_h}{I_1} \quad (19)$$

where V_1 and V_h are the rms values of the fundamental and hth harmonic voltages at the PCC and I_1 and I_h denote the rms values of the fundamental and hth harmonic line currents.

Regarding fundamental frequency active and fundamental frequency apparent powers, $P_1 = V_1 I_1 \cos(\theta_1)$ and $S_1 = V_1 I_1$ [6, 21], displacement power factor measured at the PCC, DPF(%), is found as:

$$\text{DPF}(\%) = 100\frac{P_1}{S_1} \quad (20)$$

Under the distorted current conditions, according to IEEE std. C.57.110 [32, 33], for dry-type transformers, the maximum rms current in pu and maximum loading capacity, $I_{\max}$ (pu) and $S_{\max}(\%)$, can be calculated using Eqs. (21) and (22):

$$I_{\max}(\text{pu}) = \sqrt{\frac{1 + P_{\text{ec}-R}(\text{pu})}{1 + F_{\text{HL}} P_{\text{ec}-R}(\text{pu})}} \quad (21)$$

$$S_{\max}(\%) = V_R(\text{pu}) I_{\max}(\text{pu}).100 \quad (22)$$

In these equations, $P_{\text{ec}-R}(\text{pu})$ is the eddy current loss at the fundamental frequency in pu, $V_R(\text{pu})$ denotes rated voltage of the transformer in pu, and F_{HL} is the harmonic loss factor index defined in IEEE std. C.57.110 as follows:

$$F_{\text{HL}} = \frac{\sum_h h^2 I_h^2}{\sum_h I_h^2} \quad (23)$$

In addition, the winding loss of the transformer (ΔP_T), the passive filter's loss (ΔP_{pF}), and the fundamental frequency loss of the active filter (ΔP_{aF}) can be calculated using Eqs. (24)–(26), respectively:

$$\Delta P_T = \sum_h I_h^2 R_{\text{Th}} \quad (24)$$

$$\Delta P_{\text{pF}} = \sum_h I_{\text{pFh}}^2 R_F \quad (25)$$

$$\Delta P_{\text{aF}} = |V_{L1} I_{\text{aF1}} \cos(\theta_{\text{LaF1}})| \quad (26)$$

In Eq. (26), θ_{Laf1} is the phase angle difference between the fundamental frequency load voltage and the fundamental frequency current injected by the active filter.

The investment costs (IC_{pF} and IC_{aF}) for the passive and active filters included in the hybrid filter can be written as follows [6]:

$$\text{IC}_{\text{pF}} = Q_{\Sigma C} \cdot U_C + Q_{\Sigma L} \cdot U_L \quad (27)$$

$$\text{IC}_{\text{aF}} = I_{\text{aFR}} \cdot U_{\text{aF}} \quad (28)$$

where $Q_{\Sigma C}$ and $Q_{\Sigma L}$ denote the power ratings of the capacitors and inductors used in the passive filter, while I_{aFR} is the current rating of the active filter:

$$Q_{\Sigma C} = 3 I_{\text{pF1}}^2 X_{\text{CF}} \quad (29)$$

$$Q_{\Sigma L} = 3 I_{\text{pF1}}^2 X_{\text{LF}} \quad (30)$$

$$I_{\text{aFR}} = \sqrt{\sum_h I_{\text{aFh}}^2} \quad (31)$$

In these equations, U_C and U_L are the costs per kVA of the capacitors and inductors, and U_{aF} is the cost per Amper of the active filter, respectively. In the analysis, according to the best knowledge of the authors about prices in the market, U_C, U_L, and U_{aF} are taken as 3.25 Euro/kVar, 44 Euro/kVar, and 100 Euro per Amper.

The sum of IC_{pF} and IC_{aF} gives the total investment cost of the hybrid filter:

$$\text{IC} = \text{IC}_{\text{pF}} + \text{IC}_{\text{aF}} \quad (32)$$

Based on the modeling considerations and expressions presented up to here, the formulation of the optimal design problem will be detailed and solved in the following sections.

3 Proposed optimal design approach

In this section, the problem formulation of the proposed optimal design approach is first presented. Then, a brief overview of the PSO and GA methods, which are used to solve the formulated problem, is given.

3.1 Problem formulation

This paper aims to optimally design a hybrid active filter, comprising a shunt active filter and a single-tuned shunt passive filter, to cost-effectively maximize the transformer's permissible loading capacity ($S_{\max}$) under distorted current conditions. To this end, the minimization of both the harmonic loss factor (F_{HL}) index and the filter's investment cost (IC) are handled as objectives of the optimal design problem. The minimization of the fundamental frequency loss of the active filter is considered as a third objective for its efficient operation.

The optimal design variables of the passive filter part of the hybrid filter include the capacitive reactance (X_{CF}), the tuning harmonic order (h_t), and the quality factor (Q). In addition, the parameters β and G_{e}, which define the reactive current synthesized by the active filter part, are also treated as optimization variables. All these design variables are simultaneously optimized in the considered approach.

Regarding IEEE standard 519, the constraints of the considered optimal design problem are defined as the individual ($\max V_h$ and $\max I_h$) and total harmonic distortion limits (maxTHDV and maxTHDI) of the PCC voltage and line current and the desired displacement power factor interval (95% (lagging) $\leq$ DPF $\leq$ 100%). In addition to that, to ensure a balance between harmonic selectivity and resistive losses in the single-tuned passive filter, the quality factor (Q) range is considered as the last constraint. By regarding [28, 29], the lower and upper bounds of Q are set to 30 and 60, respectively.

According to these objectives and constraints, the formulation of the optimal filter design can be written as in Eqs. (33)–(39):

Find: Hybrid filter parameters (hfp),

$$\text{To minimize } \mathrm{Of(hfp)} = m_1 F_{\mathrm{HL}}(\mathrm{hfp}) + m_2 \mathrm{IC(hfp)} + m3 \Delta P_{\mathrm{aF}}(\mathrm{hfp}) \tag{33}$$

$$\text{subjected to : } V_h(\mathrm{hfp}) \leq \max V_h \tag{34}$$

$$I_h(\mathrm{hfp}) \leq \max I_h \tag{35}$$

$$\mathrm{THDV(hfp)} \leq \mathrm{maxTHDV} \tag{36}$$

$$\mathrm{THDI(hfp)} \leq \mathrm{maxTHDI} \tag{37}$$

$$95\%(\mathrm{lagging}) \leq \mathrm{DPF(hfp)} \leq 100\% \tag{38}$$

$$30 \leq Q \leq 60 \tag{39}$$

where MaxTHDI and MaxTHDV refer to total harmonic distortion limits for current and voltage, while MaxV_h and MaxI_h are the individual harmonic distortion limits, all of which are specified in IEEE Std. 519. In addition, m_1, m_2, and m_3 denote the weighting factors assigned to the three objectives. hfp denotes all design parameters of the hybrid filter, comprising the passive filter parameters (X_{CF}, h_t, Q) and the active filter parameters (β, G_{e}).

To obtain the optimal solutions in this study, the weighting factors m_1, m_2, and m_3 are set to 0.5500, 0.3600, and 0.0900, respectively, based on the priorities of the three objectives. In the objective function, IC and ΔP_{aF} are expressed in thousands of euros (k€) and kW, respectively.

3.2 Solution algorithms

The abovementioned optimal design problem is solved using the PSO algorithm, one of the oldest and most widely used meta-heuristic algorithms [6]. To show the validity of the results, the problem is also solved by GA. The principles of both techniques are briefly summarized below. Readers are referred to [22, 23] for detailed information on both algorithms.

3.2.1 PSO algorithm

The PSO algorithm is a stochastic optimization technique that was developed by Dr. Eberhart and Dr. Kennedy in 1995 [6]. It is based on bird swarms that communicate with each other, for instance, to find food. In this algorithm, each bird represents a candidate solution, and all birds in the group together are called a "swarm." The algorithm identifies the optimal solution by evaluating the fitness function output. Each particle's velocity and position are randomly initialized. Subsequently, both parameters are iteratively updated using stochastic components and mathematical rules involving the global best (g_{best}) and personal best (p_{best}) positions [6, 22]. The velocity values are accelerated over the *gbest* and *pbest* values by using the following equations:

$$v_{id}{}^{k+1} = w \cdot v_{id}{}^{k} + c_1 \cdot U \cdot \left(pbest_{id}{}^{k} - x_{id}{}^{k}\right) + c_2 \cdot U \cdot \left(gbest_{d}{}^{k} - x_{id}{}^{k}\right) \tag{40}$$

$$x_{id}{}^{k+1} = x_{id}{}^{k} + v_{id}{}^{k+1} \tag{41}$$

where d denotes a column vector in m-dimension (d = 1; 2;...; m); i denotes a row vector in the n-dimension (i = 1;

2;…;n); k is the iteration number; vid^k is the velocity value of ith agent at the kth iteration; xid^k is the current position of the ith agent at the kth iteration; $pbest^k$ is the personal best value of the ith agent at the kth iteration; $gbest^k$ is the global best value of the ith d agent at the kth iteration; U is the random value between 0 and 1; w is the inertia weight; and c_1 and c_2 are the weighting factors, which are selected as 2 in this study.

w decreases in the interval as given in the following equation:

$$w = w_{\max} - \frac{w_{\max} - w_{\min}}{\text{iter}_{\max}} \cdot \text{iter} \tag{42}$$

The PSO algorithm is run in the Matlab environment with a swarm size of 400. The algorithm is executed 25 times, and the best result is selected as the optimal solution.

3.2.2 Genetic algorithm

Genetic algorithm (GA) is a heuristic optimization method drawn from natural selection processes, commonly utilized for addressing intricate optimization issues [23, 24]. It functions by utilizing three essential genetic operators: selection, crossover, and mutation. Given an objective function $f(x)$, the fitness of each individual in the population is evaluated, guiding the selection process. The next generation is formed by applying crossover and mutation, which introduce genetic diversity. The optimization process can be formulated as follows:

$$P(t+1) = \text{mutate}(\text{crossover}(\text{select}(P(t)))) \tag{43}$$

where $P(t)$ represents the population at generation t. The selection probability p_i of an individual i is typically proportional to its fitness:

$$p_i = \frac{f(x_i)}{\sum_j f(x_i)} \tag{44}$$

GA is implemented in Matlab environment to find the optimum solution by applying a population size and generation as 400 and 100. The algorithm is executed 25 times, and the best result is selected as the final solution.

4 Numerical results

To obtain the numerical results for the system illustrated in Fig. 1, the utility-side parameters are predetermined as follows: The fundamental frequency line-to-line background voltage is 6345 V, the short-circuit power is 210 MVA, and the total harmonic distortion of the background voltage is 1.65%. The short-circuit resistance and reactance parameters of the system, R_S and X_S, are 0.0189 Ω and 0.189 Ω, respectively. The resistance and fundamental frequency reactance of the load seen from the primary side of the transformer, R_L and X_L, are 13.85 Ω and 13.18 Ω, respectively. The consumer has a 2 MVA, star/star connected, 6300 V/400 V dry-type transformer. The harmonic model of the transformer is taken from the study [13]. Two harmonic distortion scenarios are considered for the numerical analysis. For these cases, the phasor values of the background voltage and load current harmonic sources in the equivalent circuit of the system are presented in Table 1. The power quantities and power quality indices calculated for the respective cases are given in Table 2.

Table 1 Spectrums of the background voltage and load current harmonic sources in the equivalent circuit of the system for Cases I and II

h	$\overline{I}_{\text{NLh}}$(A)		$\overline{V}_{\text{Sh}}$(V)
	Case I	Case II	
5	$14.30\angle 5 \cdot -45°$	$28.60\angle 5 \cdot -45°$	$36.64\angle 0°$
7	$13.20\angle 7 \cdot -45°$	$26.40\angle 7 \cdot -45°$	$27.48\angle 0°$
11	$12.10\angle 11 \cdot -45°$	$24.20\angle 11 \cdot -45°$	$23.82\angle 0°$
13	$11.00\angle 13 \cdot -45°$	$22.00\angle 13 \cdot -45°$	$20.15\angle 0°$
17, 19, 23, 25	$7.70\angle h \cdot -45°$	$15.40\angle h \cdot -45°$	$11.00\angle 0°$
29, 31, 35, 37	$5.50\angle h \cdot -45°$	$11.00\angle h \cdot -45°$	$3.66\angle 0°$
41, 43, 47, 49	$3.30\angle h \cdot -45°$	$6.60\angle h \cdot -45°$	$1.85\angle 0°$

Table 2 Power quantities and power quality indices for Cases I and II of the system without filtering

Indices	Case I	Case II
P_1 (kW)	1410	1410
THDV (%)	3.450	6.208
THDI (%)	16.190	32.495
DPF (%)	70.510	70.510
F_{HL}	10.345	35.710
$S_{\max}$ (%)	60.278	36.541
ΔP_{Tr} (kW)	36.462	107.160

Note that to demonstrate the advantages of optimal hybrid active filtering in improving capability for F_{HL} or $S_{\max}$ compared to optimal passive harmonic filtering, the first case (Case I) is taken from [6]. Reference [6] shows that for this case, since the single-tuned filter does not provide the current harmonic distortion levels compatible with IEEE standard 519, it cannot achieve an optimal solution for the F_{HL} minimization objective. In addition, a second case (Case II), which has a current harmonic distortion worse than Case I, is chosen to investigate the impact of an increase in current harmonic distortion on the performance of the optimal hybrid active filter design.

For both cases, P_1 and DPF are 1410 kW and 70.51%. In Case I, the THDI, $F_{HL,}$ and THDV are 16.190%, 10.345 and 3.450%, respectively. These quantities increase to 32.495%, 35.710 and 6.208% in Case II, respectively. S_{max} is calculated as 60.278% for Case I and 36.541% for Case II. These numerical results indicate that, under the simulated conditions, the transformer's maximum loading capability is significantly limited, and reactive power compensation is required. Additionally, the THDI and THDV limits defined by IEEE Std. 519 are 15% and 5%, respectively, for both cases. Therefore, it can be stated that the THDI in Case I does not comply with the standard, while both the THDI and THDV in Case II exceed the permissible limits.

The individual harmonic distortions of the PCC voltages and line currents are plotted in Figs. 4 and 5. According to the individual current harmonic limits defined by IEEE std. 519, as given in Table 3, the individual line current harmonics in both cases do not meet the permissible levels. However, in both system cases, individual voltage harmonic distortions are within acceptable limits.

4.1 Numerical results obtained for the proposed approach

This subsection is aimed at evaluating the optimal parameters of the hybrid active filter designs and the achieved values of power quality indices and losses via these filters, for the two considered cases. It should be underlined that the optimal solutions are provided by PSO and GA techniques. The solutions of PSO are given in Tables 4 and 5.

It can be mentioned from these two tables that for Cases I and II, the passive parts of the optimized hybrid filters have X_{CF} values of 27.799 Ω and 27.883 Ω. These values are very close to the capacitive reactance value required for unity power factor compensation at the fundamental frequency. Thus, one can see that the passive filter parts achieve a DPF value of 99.944%. This considerably reduces the optimal size of the active filter and the investment cost of the hybrid compensation. Additionally, for both cases, the passive filters have X_{LF} values of 0.0533 Ω and 0.1373 Ω, and they are optimally tuned to the high-order harmonics, $h_t = 22.848$ and 14.252. As a result, they significantly reduce the F_{HL} index. This contrasts with conventional passive filter designs that aim to minimize THDI because they are tuned to the dominant current harmonics, which are typically at lower frequencies. It can be mentioned from the comparative evaluation of the results obtained for Cases I and II that a higher THDI level of the load leads to a lower tuning harmonic order of the passive filter. This case can be interpreted as under higher THDI levels, the elimination of dominant current harmonics at lower harmonic orders by the passive filter becomes inevitable for a cost-effective design of the hybrid filter. Accordingly, as the THDI level increases, the passive filter's tuning harmonic order decreases. Lastly, the Q values of the optimized hybrid filters are around 30, and they have R_F values of 0.0406 Ω and 0.0652 Ω. Thus, their losses (ΔP_{pF}) are 2.318 kW and 4.069 kW for Cases I and II. It means that a higher THDI level (Case II) of the load results in a higher ΔP_{pF}. This occurs because, for the higher THDI level, the passive filter is tuned to lower harmonic order and eliminates high-amplitude current harmonics.

On the other hand, for Cases I and II, the rated currents (I_{aFR}) of the active filters in the optimally designed hybrid filters are 34.006 A and 59.364 A, respectively. The optimal β values corresponding to these current ratings are 0.788 and 0.874. One can see from these results that a higher *THDI* level of the load requires a larger size of the active filter part. The adjusted G_e values are approximately 38 mS, and ΔP_{aF} has negligible values for Cases I and II.

Using the optimal hybrid active filters, the achieved *OF* values are 3.646 and 4.636 for the first and second cases. Accordingly, F_{HL} and S_{max} values are improved to 1.271 and 98.162% for Case I, and 1.276 and 98.117% for Case II. For the respective cases, utilizing the optimized hybrid filters, ΔP_{Tr} decreases to approximately 7.700 kW. It should be noted that although there is a significant difference between the F_{HL} values (10.345 and 35.710) of the uncompensated system cases, with the support of the active filter part, the achieved F_{HL} or S_{max} values after the optimal hybrid compensation are very close to each other. On the other hand, the cost of the active filter part for Case II ($IC_{aF} = 5.936$ k€) is significantly higher than the cost of the active filter part for Case I ($IC_{aF} = 3.400$ k€). However, this is not the case for the passive filter part. As a result, the optimized total costs of the hybrid filter for Cases I and II are attained as 8.185 k€ and 10.926 k€.

From the abovementioned numerical results, it can be summarized that for Case I, the proposed hybrid filter reduces total current harmonic distortion (THDI) by 60.9%, total voltage harmonic distortion (THDV) by 49.2%, and F_{HL} by 87.7%, while increasing transformer loading capacity by 62.9%. For Case II, THDI is reduced by 82.7%, THDV by 72.0%, and F_{HL} by 96.4%, with transformer loading capacity improved by 168.5%. All these improvement levels clearly demonstrate the filter's effectiveness and cost-efficiency.

For two analysis cases, the individual harmonic distortions of the PCC voltages and line currents after filtering are plotted in Figs. 6 and 7. One can see from these two figures and Table 3 that the individual distortion levels achieved by the optimized hybrid active filters for both analysis cases are compatible with the individual harmonic distortion limits provided by the IEEE standard 519.

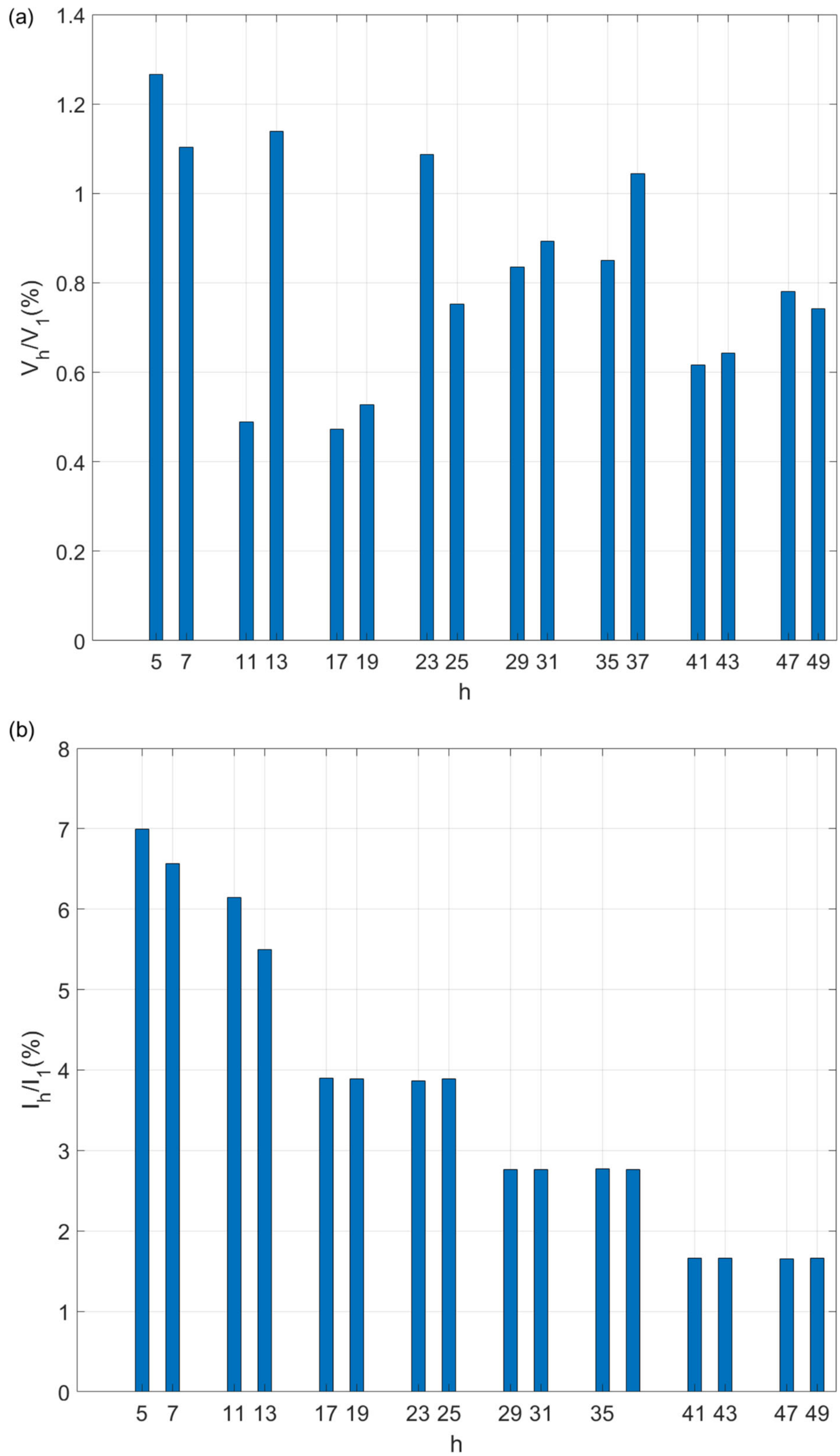

Fig. 4 The individual harmonic distortions of **a** PCC voltage and **b** line currents for Case I of the system without filtering

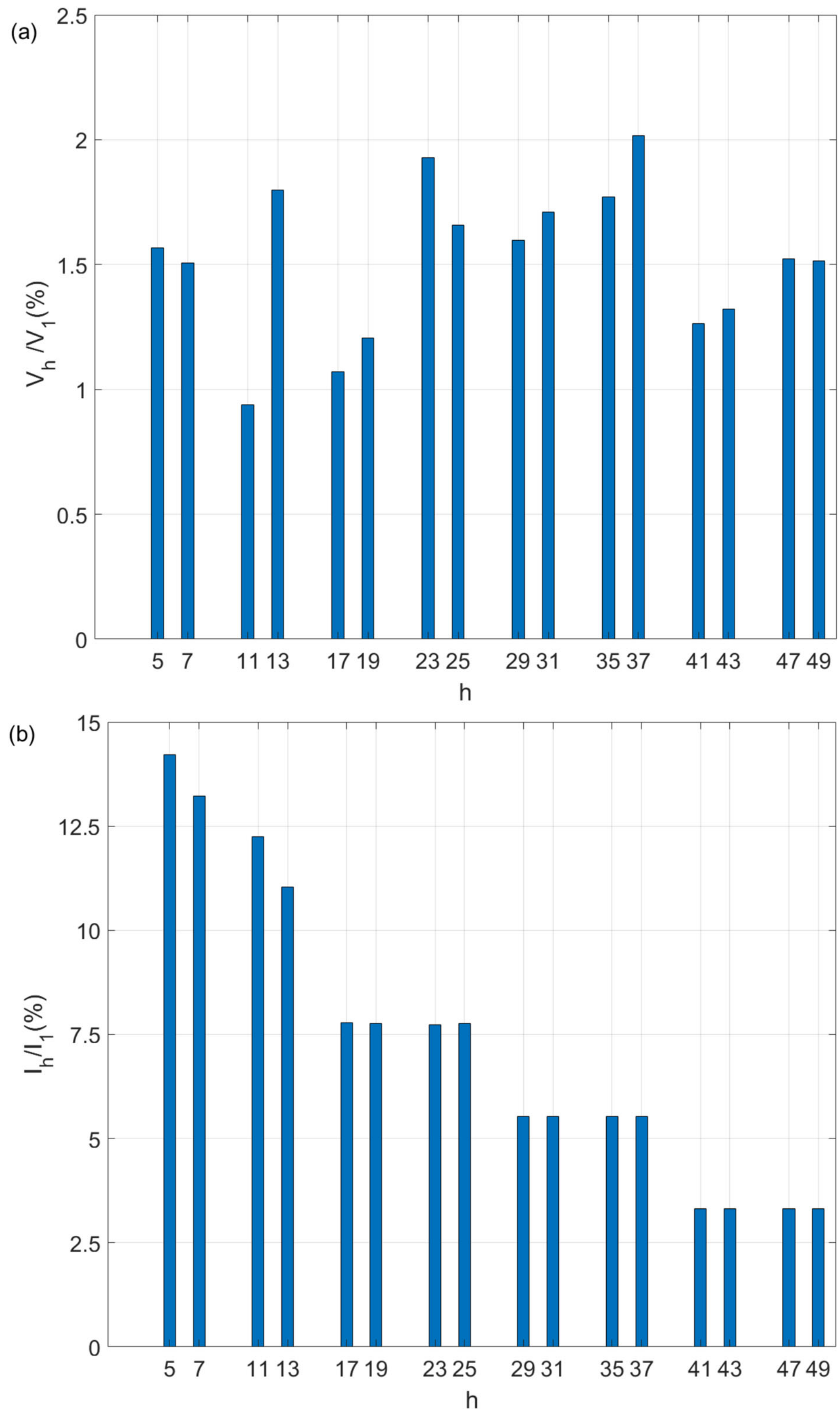

Fig. 5 The individual harmonic distortions of **a** PCC voltages and **b** line currents for Case II of the system without filtering

Table 3 The individual harmonic distortion limitations provided by the IEEE standard for the simulated system

	$h < 11$	$11 \leq h < 17$	$17 \leq h < 23$	$23 \leq h < 35$	$35 \leq h$
Line current ($I_h/I_1\%$)	12.0	5.5	5.0	2.0	1.0
PCC voltage ($V_h/V_1\%$)	3.0				

Table 4 Results of the optimal solution provided by PSO for Case I

Filter parameters		PQ indices and losses		Objectives	
X_{CF} (ohm)	27.799	THDV (%)	1.753	IC_{pF} (k€)	4.785
h_t–X_{LF} (ohm)	22.848–0.0533	THDI (%)	6.330	IC_{aF} (k€)	3.400
Q–R_F (ohm)	30.003–0.0406	DPF (%)	99.944	IC (k€)	8.185
β	0.788	F_{HL}	1.271	ΔP_{aF} (kW)	0.005
G_e (mS)	37.941	ΔP_{Tr} (kW)	7.727	S_{max} (%)	98.162
I_{aFR} (A)	34.006	ΔP_{pF} (kW)	2.318	OF	3.646

Table 5 Results of the optimal solution provided by PSO for Case II

Filter parameters		PQ indices and losses		Objectives	
X_{CF} (ohm)	27.883	THDV (%)	1.736	IC_{pF} (k€)	4.990
h_t–X_{LF} (ohm)	14.252–0.1373	THDI (%)	5.627	IC_{aF} (k€)	5.936
Q–R_F (ohm)	30.000–0.0652	DPF (%)	99.944	IC (k€)	10.926
β	0.874	F_{HL}	1.276	ΔP_{aF} (kW)	0.007
G_e (mS)	37.973	ΔP_{Tr} (kW)	7.741	S_{max} (%)	98.117
I_{aFR} (A)	59.364	ΔP_{pF} (kW)	4.069	OF	4.636

Finally, to validate the effectiveness of the optimal solutions obtained through PSO, the corresponding results derived from the GA are presented in Tables 6 and 7. A comparison of Tables 4, 5, 6 and 7 reveals that both algorithms yield hybrid filter configurations that are closely aligned. These filters demonstrate comparable performance in terms of power quality improvement and the enhancement of transformer loading capacity while also incurring similar investment costs.

4.2 Performance evaluation of the proposed filter under variable system conditions

This subsection aims to evaluate the performance of the proposed hybrid filtering approach under the variations in the utility and consumer sides. The operation of the optimally designed hybrid filter is demonstrated using a detailed time-domain Simulink model, which provides a practical and illustrative platform for analyzing the implementation of the proposed scheme.

4.2.1 Simulink modeling of the studied system

To evaluate the performance of the proposed optimal hybrid filter under varying short-circuit impedances and loading conditions, a time-domain model of the system in Simulink has been developed, as shown in Fig. 8. It represents a single-phase equivalent of the system and includes detailed submodels for the source side, transformer, load group, active filter, and passive filter.

In the Simulink model, the distorted background voltage and load current harmonics under the rated system conditions are applied based on the harmonic spectrum of Case II in Table 1, using controlled voltage and current sources. Additionally, as mentioned before, R_S and X_S are 0.0189 Ω and 0.189 Ω, respectively, and R_L and X_L are 13.85 Ω and 13.18 Ω, respectively. To prevent numerical issues during simulation, two very high-value resistors, both labeled R, are placed in parallel with the controlled current sources. For the analysis on the system's variation cases, the passive filter has optimal X_{CF}, X_{LF} and R_F parameters obtained via PSO algorithm for Case II, 27.883, 0.1373, and 0.0652 Ω. Besides, the passive filter may be disconnected from the system using a circuit breaker.

Figure 9a shows the equivalent short-circuit model of the transformer in the time domain, and it includes a resistance associated with the dc losses of the windings, short-circuit reactance, and a controlled voltage source which represents the voltage across the resistance (R_{ec}) associated with the eddy current losses. In Fig. 9b, Fourier block measures the maximum value ($\widehat{I}_{sh}$) and phase angles (α_h) of the source current, $i_s(t)$, and the function block generates the voltage signal for the controlled source based on Eq. (45).

$$v_{ec}(t) = \sum_{h \geq 1} h^2 R_{ec} \widehat{I}_{sh} \sin(\omega_h t + \alpha_h) \tag{45}$$

In the Simulink model, the current injected by the active filter is generated using the block diagram given in Fig. 10. The time-domain expression of the injected current can be

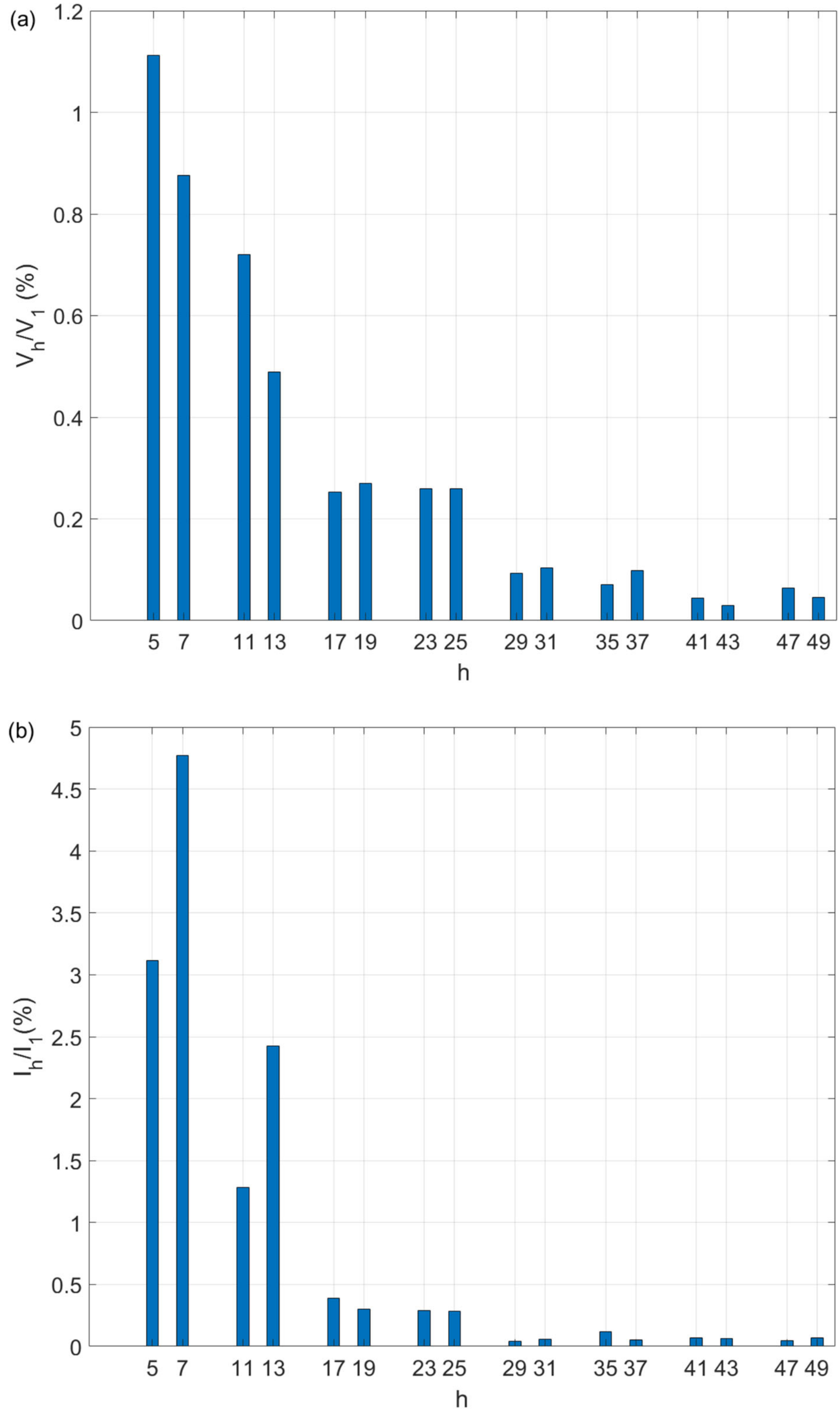

Fig. 6 The individual harmonic distortions of **a** PCC voltage and **b** line currents for Case I of the system with the filtering

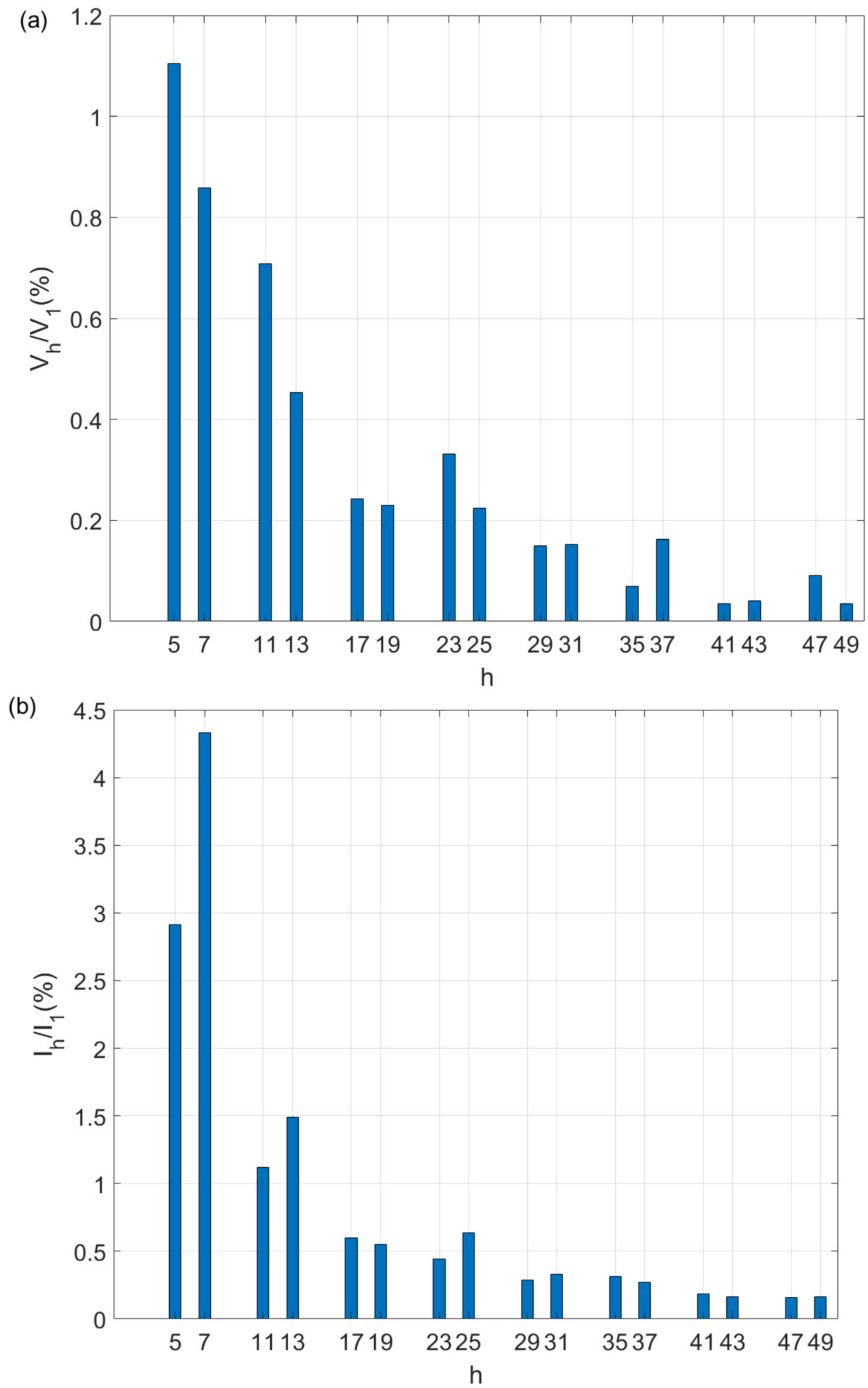

Fig. 7 The individual harmonic distortions of **a** PCC voltage and **b** line currents for Case II of the system with the filtering

written as follows:

$$i_{\mathrm{aF}}(t) = a \cdot \left(i_L(t) - \frac{P}{V_L^2} v_L(t) \right) \tag{46}$$

In this equation, as can be seen from Figs. 8 and 10, $i_L(t)$ is the current passing through the load group and passive filter, $v_L(t)$ and V_L are the instantaneous and RMS values of the load bus voltage, and P denotes the active power consumed by the load group and passive filter. The variable a serves as a limiter, keeping the RMS value of i_{aF}(t) within the optimized rated current of the active filter ($I_{aFR} = 59.364$ A). If the RMS value of $i_{aF}(t)$ is less than or equal to I_{aFR}, then a is equal to 1. Otherwise, a takes a real value less than 1 that

Table 6 Results of the optimal solution provided by GA for Case I

Filter parameters		Power quality indices and losses		Objectives	
X_{CF} (ohm)	27.790	THDV (%)	1.765	IC_{pF} (k€)	4.761
h_t–X_{LF} (ohm)	25.304–0.0434	THDI (%)	6.563	IC_{aF} (k€)	3.402
Q–R_F (ohm)	30.001–0.0366	DPF (%)	99.944	IC (k€)	8.163
β	0.782	F_{HL}	1.291	ΔP_{aF} (kW)	0.002
G_e (mS)	37.936	ΔP_{Tr} (kW)	7.756	S_{max} (%)	97.985
I_{aFR} (A)	34.019	ΔP_{pF} (kW)	2.097	OF	3.649

Table 7 Results of the optimal solution provided by GA for Case II

Filter parameters		Power quality indices and losses		Objectives	
X_{CF} (ohm)	27.874	THDV (%)	1.757	IC_{pF} (k€)	4.968
h_t–X_{LF} (ohm)	14.741—0.1283	THDI (%)	6.153	IC_{aF} (k€)	5.909
Q–R_F (ohm)	30.002—0.0630	DPF (%)	99.944	IC (k€)	10.878
β	0.863	F_{HL}	1.312	ΔP_{aF} (kW)	0.116
G_e (mS)	37.973	ΔP_{Tr} (kW)	7.795	S_{max} (%)	97.809
I_{aFR} (A)	59.092	ΔP_{pF} (kW)	3.972	OF	4.648

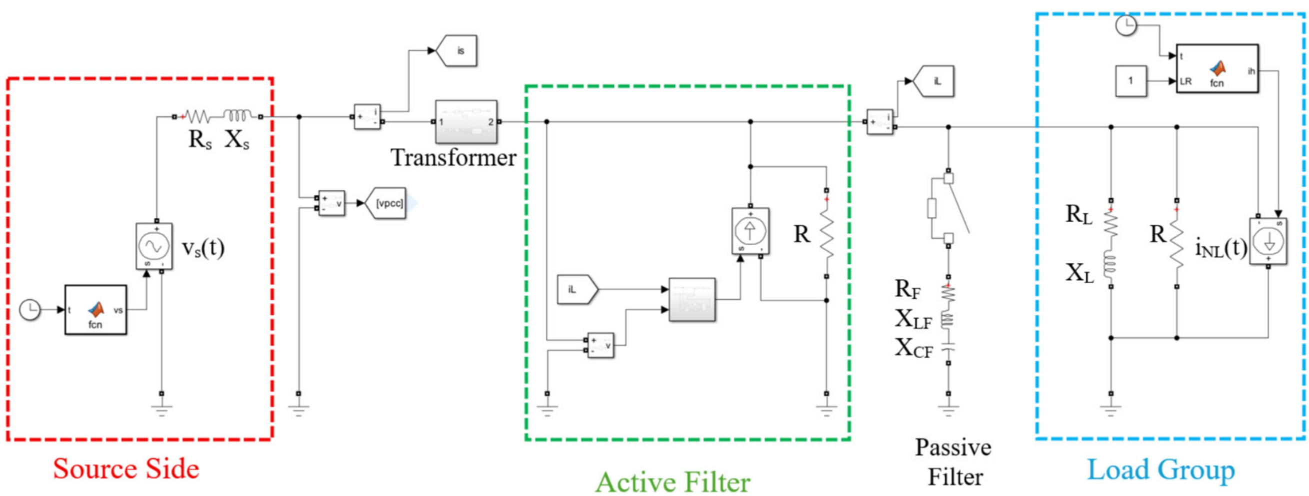

Fig. 8 Simulink modeling of the studied system in time domain

Fig. 9 Simulink modeling of the transformer in time domain

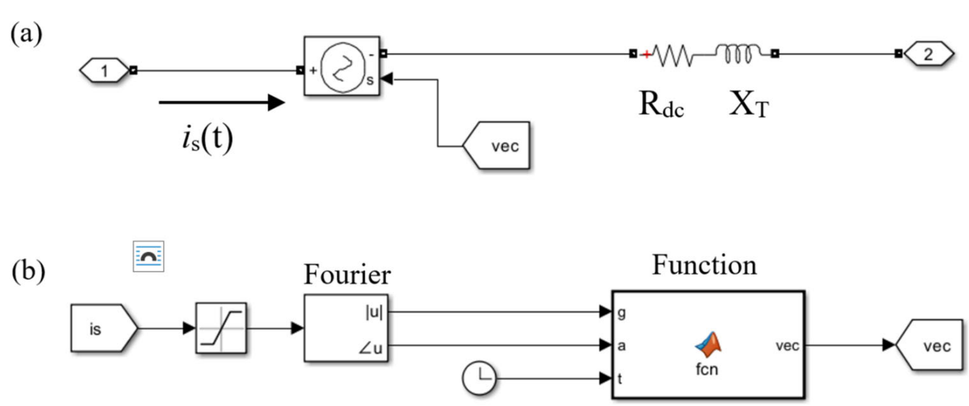

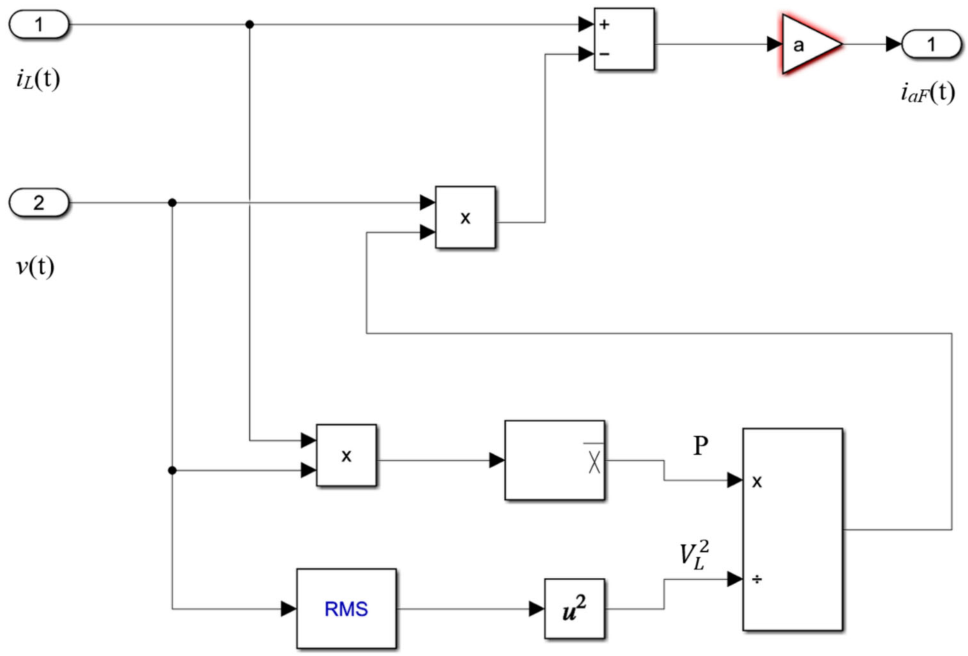

Fig. 10 Active filter current generation blocks

limits the RMS value of $i_{aF}(t)$ to I_{aFR}. In the simulations, a is determined through a trial-and-error approach.

4.2.2 Results for variable loading cases

It is well established in the literature that passive filters tend to exhibit poor performance under low-loading conditions [6]. To investigate the impact of consumer-side load variations on the proposed filter performance, the loading level is treated as a variable parameter in this study. Furthermore, to avoid the inefficiencies associated with the passive component at low loading, the proposed hybrid filter can be operated such that only its active part is utilized under these conditions.

To determine the loading range within which the active component alone is sufficient to meet harmonic distortion limits and reactive power compensation requirements, the parameters THDV, THDI, $S_{\max}$, and DPF are evaluated across variable loading conditions. For the simulations, it is assumed that under varying loading conditions ranging from the rated level (100%) down to 20%, the resistance (R_L) and reactance (X_L) representing the linear load increase inversely with the loading level. Simultaneously, the magnitudes of the harmonic current sources (I_{NLh}), modeled in parallel with the linear load impedance, are assumed to decrease directly proportional to the loading level. Throughout the analyses, both the power factor of the load and the phase angles of the load's harmonic current components are considered constant.

The corresponding results, simulated for the system's worst-case scenario (Case II), are depicted in Figs. 11 and 12.

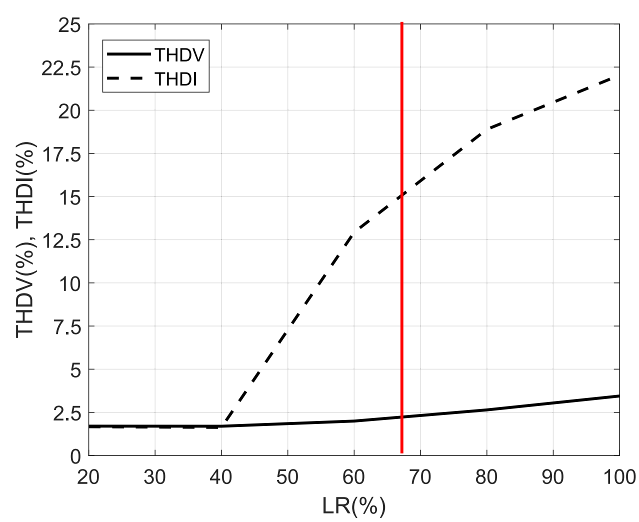

Fig. 11 The variation of THDV and THDI levels achieved using only the active part of the proposed filter design for the loading levels between 20 and 100%

In Fig. 11, the vertical red line indicates the system's THDI limit of 15%. The results show that the active filter maintains current harmonic distortion within IEEE 519 standards for loading levels between 20 and 68%. Additionally, the figure confirms that, for all loading levels, the voltage distortion at the point of common coupling (THDV) remains below the IEEE threshold of 5%.

Figure 12 presents the DPF and transformer loading capability. Here, the vertical red line denotes the minimum acceptable DPF (95% lagging), while the blue vertical line marks the loading level limit which the transformer cannot

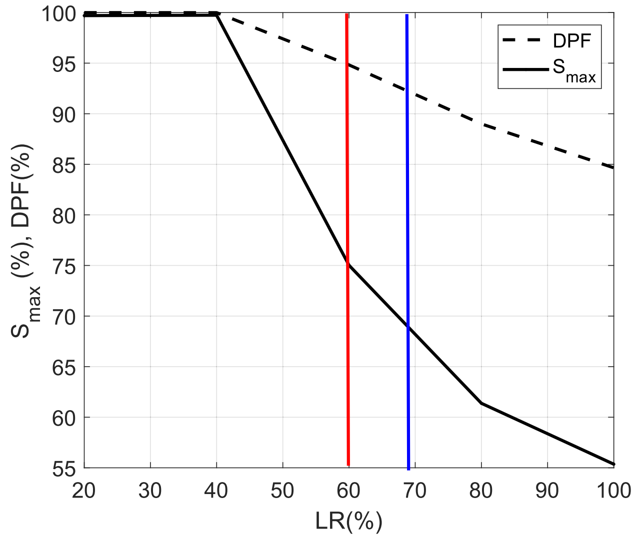

Fig. 12 The variation of S_{max} and DPF values achieved using only the active part of the proposed filter design for the loading levels between 20 and 100%

Table 8 For the loading levels such as 65%, 75% and 85%, the THDV, THDI, DPF, and S_{max} values achieved using the optimized hybrid filter

	LR = 65%	LR = 75%	LR = 85%
THDV (%)	1.818	1.778	1.789
THDI (%)	6.994	4.572	4.260
DPF (%)	99.906	99.999	99.990
S_{max} (%)	96.878	98.521	98.794

operate safely. The figure reveals that the active filter alone achieves DPF values exceeding 95% up to a 60% loading level. Moreover, it allows safe operation of the transformer at loading levels up to 68%.

Hence, it can be stated that for loading levels up to 60%, the active component of the hybrid filter alone is sufficient to improve the transformer's loading capacity while also fulfilling the requirements for harmonic mitigation and reactive power compensation. For higher loading levels—specifically at 65%, 75%, and 85%—the performance of the optimized hybrid filter is presented in Table 8. The values of THDV, THDI, DPF, and S_{max} are recorded as follows:

- At 65% loading: 1.818%, 6.994%, 99.906%, and 96.878%
- At 75% loading: 1.778%, 4.572%, 99.999%, and 98.521%
- At 85% loading: 1.789%, 4.260%, 99.990%, and 98.794%

These results demonstrate that for higher loading levels, the optimized hybrid filter effectively meets harmonic distortion and reactive power requirements while enabling increased transformer loading.

Table 9 Power quality indices variations with different short-circuit capacities

	S_{SC} = 424 MVA	S_{SC} = 141 MVA
THDV (%) (without filter)	3.576	9.389
THDV (%) (with the filter)	1.740	1.869
THDI (%) (with the filter)	5.741	5.754
DPF (%) (with the filter)	99.944	99.944
S_{max} (%) (with the filter)	97.753	97.973

Based on the results detailed up to here, a load-adaptive management strategy can be introduced to enhance the performance of the proposed hybrid filter under varying loading conditions. In this strategy, only the active filter is utilized at low loading levels, whereas both active and passive filters are activated when the loading level is higher.

4.2.3 Results for variable system impedance cases

Variations in the short-circuit impedance of the utility grid may occur due to factors such as network faults, maintenance work, system capacity expansions, or the integration of new generation and distribution equipment. These variations affect the network's short-circuit power and can, in turn, influence the harmonic distortion levels at the PCC.

This study accounts for this issue by evaluating the robustness of the optimized hybrid filter under two additional scenarios: one in which the short-circuit impedance is reduced by 50% and another in which it is increased by 50%, relative to the original system conditions. Note that for these two additional scenarios, short-circuit powers (S_{SC}) of the system are 424 MVA and 141 MVA, respectively. To achieve both cases, the ratio X_S/R_S of the impedance is kept constant and the fundamental frequency magnitude of the impedance ($\sqrt{R_S^2 + X_S^2}$) is adjusted to be inversely proportional to the short-circuit power of the system.

Thus, the corresponding THDV, THDI, DPF, and S_{max} values for the original and modified versions of Case II with hybrid filtering are presented in Table 9. For comparison, the same table also includes the unfiltered system's THDV at the PCC. As illustrated in Table 9, THDV at the PCC is highly sensitive to changes in short-circuit impedance in the absence of filtering. For the uncompensated system, the THDV values are observed as 3.576%, 6.208%, and 9.389% for the low, nominal (original), and high short-circuit impedance cases, respectively. Once the optimized hybrid filter is implemented, the THDV and THDI are reduced to approximately 1.8% and 5.7%, respectively, across all short-circuit impedance scenarios. Additionally, the DPF exceeds 99%, and S_{max} is increased beyond 97%.

These findings clearly demonstrate that the proposed hybrid filter is highly resilient to changes in grid short-circuit impedance, providing stable power quality and reliable filtering performance under varying network conditions.

5 Conclusion

This study proposed an optimally designed hybrid active filter—comprising a shunt single-tuned passive filter and a shunt active filter—to cost-effectively maximize the loading capacity of power transformers operating under harmonically distorted voltage and current conditions.

The design objective was the simultaneous minimization of the harmonic loss factor, investment cost, and the fundamental frequency loss of the active filter component, subject to IEEE standard 519 harmonic distortion limits, desired power factor interval, and quality factor range. The optimization problem was solved using both PSO and GA techniques.

Numerical results demonstrate that the active filter significantly supports the passive filter in enhancing transformer loading capacity (S_{max}) while maintaining power quality compliance. The passive component handles fundamental reactive power compensation and is optimally tuned to high-order harmonics—unlike conventional passive filters, which target dominant low-order harmonics. Although an increase in THDI level of the system leads to higher losses in the passive filter, the overall performance on the mitigation of F_{HL} and S_{max} remains consistent across cases due to the active filter's contribution. PSO and GA techniques yield hybrid filter configurations that are closely aligned. These filters demonstrate comparable performance in terms of power quality improvement and the enhancement of transformer loading capacity while also incurring similar investment costs. Lastly, from the performance analysis of the optimally designed hybrid filter under a wide range of variations in load demand and grid short-circuit impedance, it can successfully be employed in the practical systems.

The proposed design can particularly be employed in industrial facilities, renewable energy plants, and data centers, where harmonic pollution is a common power quality problem and transformer utilization should be maximized without compromising reliability. The optimization framework is flexible and can be adapted to suit various grid conditions and economic priorities.

In future works, it is planned to integrate design constraints from IEEE 18-2012 to account for capacitor reliability and thermal stress, bringing the design closer to practical deployment standards. Additionally, to test the performance of the proposed optimal hybrid filter for the practical systems in more detail, it may be necessary to perform analyses under numerous random variations on the source and load sides. The unbalanced system conditions should also be considered in the future analysis studies. In addition, the performance of the active filter part of the hybrid filter is directly affected by the uncertainties in the voltage and current measurements. The changes in the values of the passive filter elements depending on time, i.e., aging, may adversely affect the long-term performance of the hybrid filter. Therefore, the authors plan to perform the abovementioned uncertainty analyses to evaluate how the proposed hybrid filter affects the harmonic reduction and transformer loading capacity improvement performance.

In future works, beyond the simulation-based analysis, collaborations with industry partners may be explored to test the proposed design in real-world installations or employ hardware-in-the-loop (HIL) simulations for semi-physical validation. Thus, the real-world applicability and reliability of the proposed design will be further strengthened. Lastly, the performance of the optimal hybrid filter designs incorporating different passive filter topologies will be investigated.

Acknowledgements This work was conducted as part of the scientific research Project No. 2024/026 and it was funded by Balikesir University.

Author contributions MEB and AK obtained the simulation results. All authors contributed to the interpretation of the simulation results and writing of the manuscript text. MEB and SHEAA reviewed the manuscript.

Data availability No datasets were generated or analyzed during the current study.

Declarations

Conflict of interest The authors declare that they have no conflict of interest.

References

1. Cantürk Ş, Karakaya O, Erhan Balci M, Aleem SHEA (2024) Introductory chapter: effects of power quality problems on energy efficiency of power systems. Energy Efficiency of Modern Power and Energy Systems, Elsevier, pp 1–17. https://doi.org/10.1016/B978-0-443-21644-2.00001-4
2. Hu Z, Han Y, Zalhaf AS, Zhou S, Zhao E, Yang P (2023) Harmonic sources modeling and characterization in modern power systems: a comprehensive overview. Electr Power Syst Res 218:109234–109234. https://doi.org/10.1016/j.epsr.2023.109234
3. Lin B-R, Yang B-R, Tsai H-R (2002) Analysis and operation of hybrid active filter for harmonic elimination. Electr Power Syst Res 62(3):191–200. https://doi.org/10.1016/s0378-7796(02)00038-x
4. Demirdelen T, İnci M, Bayindir KÇ, Tümay M (2013) Review of hybrid active power filter topologies and controllers. In: 4th international conference on power engineering, energy and electrical drives, Istanbul, Türkiye, 13–17 May 2013, pp 587–592. https://doi.org/10.1109/PowerEng.2013.6635674
5. Barva AV, Joshi S (2022) A comprehensive survey on hybrid active power filter topologies and controller and application in microgrid. In: 2022 IEEE Region 10 symposium (TENSYMP), Mumbai, India, 01–03 July 2022, pp 1–6. https://doi.org/10.1109/TENSYMP54529.2022.9864377

6. Karadeniz A, Balci ME (2018) Comparative evaluation of common passive filter types regarding maximization of transformer's loading capability under non-sinusoidal conditions. Electr Power Syst Res 158:324–334. https://doi.org/10.1016/j.epsr.2018.01.019
7. Albatran S, Koran A, Smadi IA, Ahmad HJ (2018) Optimal design of passive RC-damped LCL filter for grid-connected voltage source inverters. Electr Eng 100(4):2499–2508. https://doi.org/10.1007/s00202-018-0725-5
8. Al-Barashi M, Meng X, Liu Z, Saeed MSR, Tasiu IA, Wu S (2023) Enhancing power quality of high-speed railway traction converters by fully integrated T-LCL filter. IET Power Electron 16(5):699–714. https://doi.org/10.1049/pel2.12415
9. Al-Barashi M, Wang Y, Lan B, Bhutta MS (2024) Magnetic integrated double-trap filter utilizing the mutual inductance for reducing current harmonics in high-speed railway traction inverters. Sci Rep 14:10058. https://doi.org/10.1038/s41598-024-60877-y
10. Al-Barashi M, Wang Y, Bhutta MS (2024) High-frequency harmonics suppression in high-speed railway through magnetic integrated LLCL filter. PLoS ONE 19(6):e0304464–e0304464. https://doi.org/10.1371/journal.pone.0304464
11. Al-Barashi M et al (2025) Magnetic integrated multi-trap filters using mutual inductance to mitigate current harmonics in grid-connected power electronics converters. Energies 18(2):423. https://doi.org/10.3390/en18020423
12. Balci ME, Karaoglan AD (2013) Optimal design of C-type passive filters based on response surface methodology for typical industrial power systems. Electr Power Components Syst 41(7):653–668. https://doi.org/10.1080/15325008.2013.763310
13. Balci ME (2014) Optimal C-type filter design to maximize transformer's loading capability under non-sinusoidal conditions. Electr Power Components Syst 42(14):1565–1575. https://doi.org/10.1080/15325008.2014.943827
14. Balci ME, Sakar S (2014) Optimal design of single-tuned passive filters to minimize harmonic loss factor. Middle-East J Sci Res 21(11):2149–2155. https://doi.org/10.5829/idosi.mejsr.2014.21.11.21665
15. Buła D, Grabowski D, Maciążek M (2022) A review on optimization of active power filter placement and sizing methods. Energies 15(3):1175. https://doi.org/10.3390/en15031175
16. Zobaa AF (2014) Optimal multiobjective design of hybrid active power filters considering a distorted environment. IEEE Trans Ind Electron 61(1):107–114. https://doi.org/10.1109/tie.2013.2244539
17. Biswas PP, Suganthan PN, Amaratunga GAJ (2017) Minimizing harmonic distortion in power system with optimal design of hybrid active power filter using differential evolution. Appl Soft Comput 61:486–496. https://doi.org/10.1016/j.asoc.2017.08.031
18. Alasali F, Nusair K, Foudeh H, Holderbaum W, Vinayagam A, Aziz A (2022) Modern optimal controllers for hybrid active power filter to minimize harmonic distortion. Electronics 11(9):1453–1453. https://doi.org/10.3390/electronics11091453
19. Zobaa AF (2007) Letter to the editor: optimal sizing of the passive filter's elements in hybrid active filters. Electr Power Components Syst 35(4):483–488. https://doi.org/10.1080/15325000601023761
20. Karadeniz A, Balci ME (2024) An optimal hybrid harmonic filter design for maximization of transformer loading capability under non-linear loading conditions. In: ICAME 2024, Ayvalik, Türkiye, 26–28 June 2024, p 98
21. IEEE recommended practice and requirements for harmonic control in electric power systems. In: IEEE Std 519-2014 (Revision of IEEE Std 519–1992), pp 1–29, June 2014. https://doi.org/10.1109/IEEESTD.2014.6826459
22. Gad AG (2022) Particle swarm optimization algorithm and its applications: a systematic review. Arch Comput Methods Eng 29(5):2531–2561. https://doi.org/10.1007/s11831-021-09694-4
23. Alhijawi B, Awajan A (2023) Genetic algorithms: theory, genetic operators, solutions, and applications. Evol Intell 17(3):1245–1256. https://doi.org/10.1007/s12065-023-00822-6
24. Katoch S, Chauhan SS, Kumar V (2021) A review on genetic algorithm: past, present, and future. Multimed Tools Appl 80:8091–8126. https://doi.org/10.1007/s11042-020-10139-6
25. Menti A, Zacharias T, Milias-Argitis J (2009) Optimal sizing and limitations of passive filters in the presence of background harmonic distortion. Electr Eng 91(2):89–100. https://doi.org/10.1007/s00202-009-0120-3
26. Abdel Aleem SHE, Balci ME, Sakar S (2015) Effective utilization of cables and transformers using passive filters for non-linear loads. Int J Electr Power Energy Syst 71:344–350. https://doi.org/10.1016/j.ijepes.2015.02.036
27. Karadeniz A, Balci ME, Hocaoglu MH (2023) Improvement of PV unit hosting capacity and voltage profile in distorted radial distribution systems via optimal sizing and placement of passive filters. Electr Eng 105(4):2185–2198. https://doi.org/10.1007/s00202-023-01800-y
28. Awadalla M, Omer M, Mohamed A (2015) Single-tuned filter design for harmonic mitigation and optimization with capacitor banks. In: 2015 international conference on computing, control, networking, electronics and embedded systems engineering (ICCNEEE), Khartoum, Sudan, 07–09 September 2015, pp 242–247. https://doi.org/10.1109/ICCNEEE.2015.7381370
29. Cho Y-S, Cha H (2011) Single-tuned passive harmonic filter design considering variances of tuning and quality factor. J Int Counc Electr Eng 1(1):7–13. https://doi.org/10.5370/jicee.2011.1.1.007
30. Salmeron P, Herrera RS (2006) Distorted and unbalanced systems compensation within instantaneous reactive power framework. IEEE Trans Power Deliv 21(3):1655–1662. https://doi.org/10.1109/tpwrd.2006.874115
31. Rafael O, Charif K, Mohamad O, Daniel S (2006) Comparison of reference current generation techniques for non-active power compensation under distorted and unbalanced conditions. IECON 2006—32nd annual conference on IEEE industrial electronics, Paris, France, 06–10 November 2006, pp 2297–2302. https://doi.org/10.1109/IECON.2006.347514
32. IEEE recommended practice for establishing liquid-immersed and dry-type power and distribution transformer capability when supplying nonsinusoidal load currents. IEEE Std C57.110-2018 (Revision of IEEE Std C57.110-2008), pp 1–68, Oct. 2018. https://doi.org/10.1109/IEEESTD.2018.8511103
33. Arslan E, Balci ME, Hocaoglu MH (2014) An analysis into the effect of voltage harmonics on the maximum loading capability of transformers. In: 2014 16th international conference on harmonics and quality of power (ICHQP), Bucharest, Romania, 25–28 May 2014, pp 616–620. https://doi.org/10.1109/ICHQP.2014.6842925